CHAPTER V

PHYSICOCHEMICAL STUDIES ON STRUCTURED AGGREGATES WITH SPECIAL REFERENCE TO IONIC LIQUID BASED SURFACTANTS

5.1. Introduction

Ionic liquids (ILs) have attracted much attention at present due to their unique physicochemical qualities. [1–4]

Ionic liquid with long hydrocarbon chain are found to active at interface and usually known as surface active ionic liquids (SAILs), special kind of useful ILs with collective properties of ILs and surfactants. [5]

ILs can be designed and tuned to optimized yield. Through the possibility of fine-tuning Hydrophobicity of the ILs by altering the hydrocarbon chain length, the type of counter group, and the nature of the anions, one can modify the structure of these molecular aggregates. [6-16]

Many of the SAILs described in the literature containing halogen. Though the SAILs are environmentally caring compare to the organic solvents still presence of halogen can release corrosive HF or HCl. [17] Nowadays lot of ionic liquids without halogen already synthesized, moreover many of them are commercialized.

Alkyl sulfate-based ILs from the previously mentioned is clearly categorized by their high practical accessibility with comparatively low cost and by their well-documented toxicology and biodegradability. [17], [18], [19], [20]

In this work, halogen-free BMIMDS and BMPDS derived from relatively inexpensive chemicals were synthesized using ion exchange, a method easier than that of the earlier literature and described elsewhere. Characterisation of the obtained product was done with melting point measurement, FT-IR, FT-NMR which validates simple and standardized synthetic methodology as well as purity of the both products. Their interfacial behaviour was studied by conductivity, surface tensiometry and steady state

fluorimetric technique. The CMC values obtained from surface tensiometry and conductometry were justified further by fluorimetry.

5.2. Experimental Section

5.2.1. Materials

1-Butyl-3-methylimidazolium chloride (BMIMCl), 1-Butyl-1-methylpyrrolidinium tetrafluoroborate ($BMPyBF_4$), Sodium dodecyl sulfate (SDS) have been used for synthesis. Double distilled water specific conductance ~0.9 μScm^{-1}, pH ~6.8–7.0 was used for all experimental purposes. The probe used for the fluorescence was pyrene. All the samples were purchased from Sigma-Aldrich.

5.2.2. Preparation:

At starting, the solubility of the chosen precursor ILs and Sodium dodecyl sulfate (SDS) have been accurately checked in the different solvent and finally dichloromethane (DCM) was chosen as a suitable solvent. The easy solvent removal was also taken into consideration. 1-Butyl-3-methylimidazolium dodecyl sulfate (BMIMDS), 1-Butyl-1-methylpyrrolidium dodecyl sulfate (BMPDS) were prepared by simple ion exchange reaction of 1-butyl-3-methylimidazoliumchloride (BMIMCl) and 1-butyl-1-methylpyrrolidiniumtetrafluoroborate ($BMPyBF_4$) respectively (SDS).

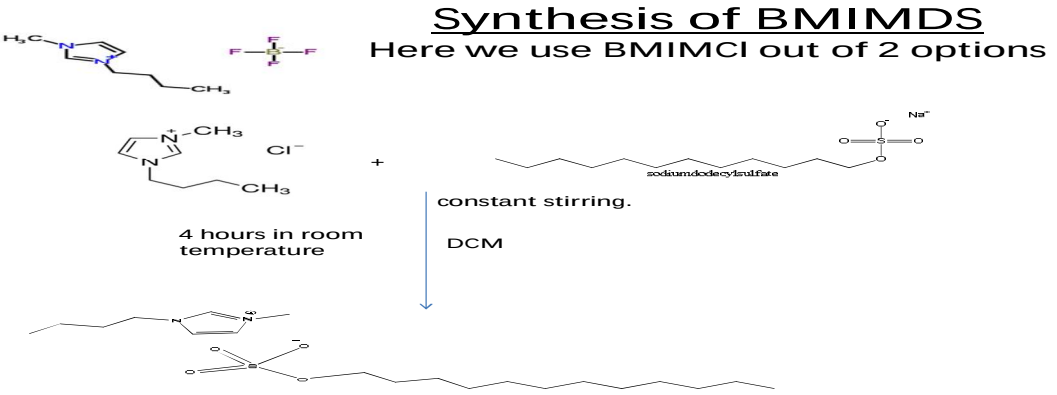

Scheme 1: Synthesis of 1-Butyl-3-methylimidazolium dodecyl sulfate (BMIMDS)

The precursors (BMIMCl and $BMPyBF_4$) with sodium lauryl sulfate in 1:1M ratio was taken in DCM and continuously stirred at room temperature for 4 & 5 h respectively. As the secondary product was ionic in nature so it was in the solid state in the organic solvent, was easily separated by careful filtration. Then the immiscible (organic) phase, which was waxy in nature, was heated in a rotary vacuum evaporator.

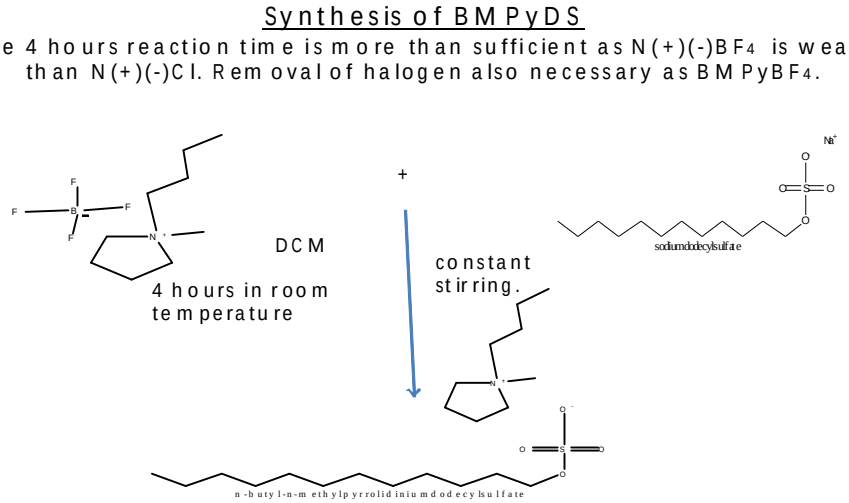

Scheme2: Synthesis1-butyl-1-methylpyrrolidium dodecyl sulfate (BMPDS)

Used volatile solvent (DCM, boiling point about 39.6°C) was removed gently by maintaining required temperature by a rotary evaporator. Then obtained coloured highly viscous liquid was washed with water very gently until the phase becomes chloride-free (the presence of the chloride was tested by $AgNO_3$ in low pH solution). The product was dried, stored in dark place and vacuum desiccators for 48 h. The aqueous

Solution which was used for halide removal was also stored to check any product accumulation in the water, has been found with negligible product accumulation.

5.2.3. Apparatus and procedure:

Fourier transform Infrared spectra (FTIR) were recorded in KBr pellets with a PerkinElmer FT-IR spectrometer (RX-1) operating in the region of 4000 to 400 cm^{-1} at ambient temperature. [21]

^{1}H Nuclear magnetic resonance (NMR) & 2D NOESY experiments were performed in BRUKER AVANCE spectrometer operating at 300 MHz frequency. [22] The respective solutions were made in D_2O, data was reported as a chemical shift.

Ultraviolet-visible (UV-visible) spectra were recorded by JASCO V-530 UV-vis Spectrophotometer, with an uncertainty of wavelength resolution of ±2 nm. The measuring temperature was controlled by an automated digital thermostat. Spectrophotometer UVD-2950 (Labomed Inc., USA) [23]

The Conductance measurements were accomplished in a Mettler Toledo Seven Multi conductivity meter with uncertainty 1.0 $\mu S\ m^{-1}$, bearing a cell constant of about (0.1 ± 0.001) cm^{-1}. Temperature of the solutions were maintained to within = (298.15± 0.01) K using Brookfield Digital TC-550 temperature thermostat bath. The used cell was calibrated using a 0.01 M aqueous KCl solution. The uncertainty in temperature was ±0.01 K. [23]

Surface tension experiments were carried out by a platinum ring detachment method using du Nou¨y Tensiometer (Jencon, Kolkata, India) and also Tensiometer (K9, KRÜSS, Germany) at the experimental temperature. The accuracy of the surface tension measurement was within 0.1 mN m^{-1}. The constant temperature was maintained during the experiments with Remi ultra thermostat (CB-700) with precision 0.1K. [24]

Steady-state fluorescence emission study was carried out in bench top spectrofluorimeter from photon technologies international (Quantamaster-40) with FelixGX version 2.0 software. [22]

Dynamic Light Scattering (DLS) was performed on a Zetasizer Nano ZS90 ZEN3690 light scattering apparatus (Malvern Instruments Ltd., Malvern, UK) with the He–Ne laser (632.8 nm, 4 mW) at a scattering angle of 90°. The temperature was maintained constant at 298.15 K. [25]

Polarizing Optical Microscopy was performed with Polarizing Microscope (Model Nikon Eclipse LV100 POL) connected with Linkam U.K Heating/Freezing Stage accessories

5.2.4. FTIR analysis of the products

The observed infrared frequencies of the bond correspond to functional groups of all the precursors and products have been shown (Fig. 1a) within the range of 500–4000 cm^{-1}.

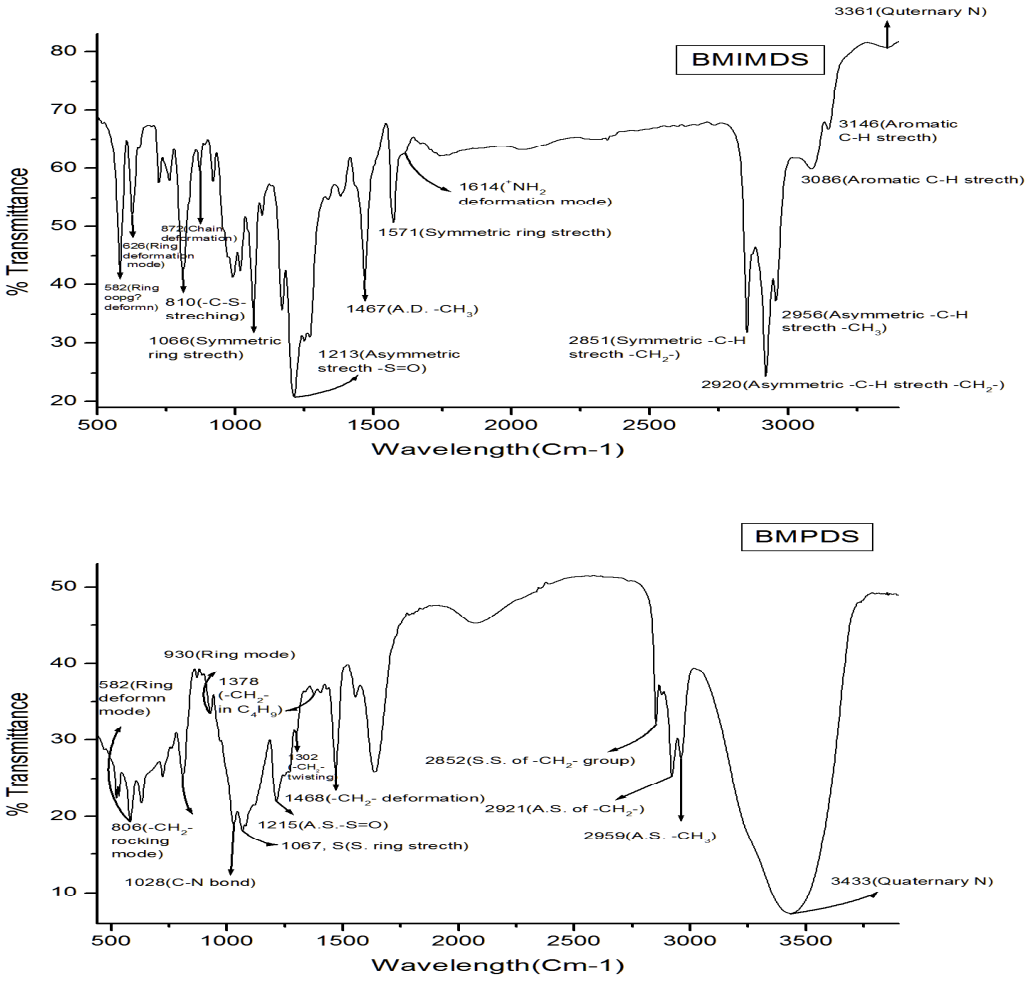

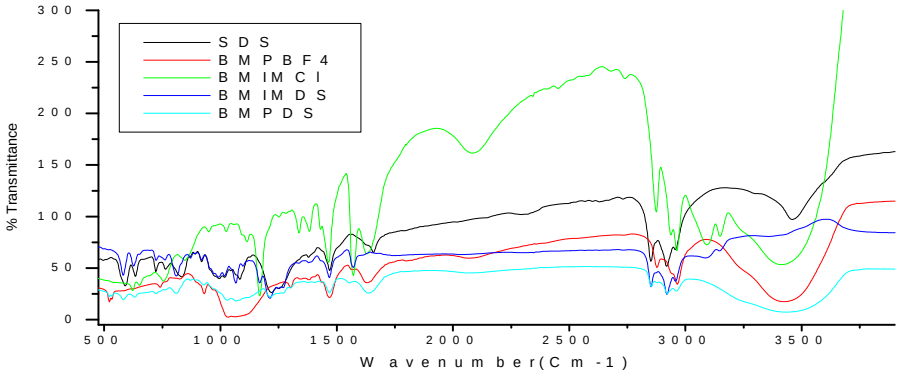

Fig. 1: FTIR spectra of BMIMDS, BMPDS & all in the same frame

Serial no.	Compound	Stretching frequency(Cm^{-1})	Functional group with bond
1	SDS	3460	-OH stretching
		2958	A.S. $-CH_3$
		2921	A.S. $-CH_2-$
		2852	S.S. $-CH_2-$
		1660	C=C stretching
		1473	$-CH_2-$ scissoring mode
		1221	A.S. S=O
		1084	SO_2 symm. vibration
2	BMIMCl	3416	Quarternary N-atom
		3151	Aromatic C-H stretching
		3095	Aromatic C-H stretching
		2971	A.S. $-CH_3$
		1631	C=C stretch.
		1571	C=N stretch
		1461	A.D. $-CH_3$/S. ring stretch
		844	-C-N- stretch

Serial no.	Compound	Stretching frequency(Cm^{-1})	Functional group with bond
3	$BMPBF_4$	3425	Quarternary N type of structure
		2967	A.S. $–CH_3$
		2878	S.S. of $–CH_2$ group
		1467	$-CH_2-$ Def. Or scissoring, connected with N-atom
		1052	C-C, BF_4 stretch
		1030	N-Bu, N-Me
4	BMIMDS	3373	Quarternary N^+ type
		3147	Aromatic C-H stretch
		3089	Aromatic C-H stretch
		2957	A.S. –C-H of CH_3
		2920	A.S. $–CH_2-$
		2853	S.S. $–CH_2-$
		1569	S. ring stretch
		1467	A.D. - CH_3/S. ring stretch
		1213	A.S. –S=O
		1068	Sym. ring stretching
		870	Chain def.
		610	-C-S- stretch[26]-[34]
5	BMPDS	3439	Quaternary amine type in pyrrolidinium cation
		3031	Aromatic -C-H bond vibration
		2954	A. S. $–CH_3$
		2919	S. S. -C-H of $-CH_2-$

Serial no.	Compound	Stretching frequency(Cm^{-1})	Functional group with bond
		2851	**S. S. $-CH_3$**
		1643	**-C=C- stretching**
		1467	**-C-H bending/ asymmetric deformation of $-CH_2-$**
		806	**-C-O-S- of $-CH_2-O-S-$ stretching**
		1213	**A.S. of the $-SO_4^{-1}$ group[26]-[34]**

Table 1: FTIR data of the BMIMCl, $BMPyBF_4$, SDS, BMIMDS and BMPDS

5.2.5. NMR analysis of the products

The treated precursors, products viz. BMIMCl, $BMPyBF_4$, SDS, BMIMDS and BMPDS were characterized by ^1H NMR spectroscopy using D_2O as a solvent on a spectrometer (Bruker Avance 300 MHz spectrometer) for the determination of molecular structures. The ^1H NMR spectra data are shown in Fig. 2. in ppm (δ) from the internal reference (D_2O: δ 4.788 ppm) in determining the proton chemical shifts. The ^1H NMR of the precursors like that: **BMIMCl in D_2O (δ/ppm)**: **7.512**(m, 2H, NCH), **4.75**(residual solvent peak), **4.234**(t, 2H, NCH_2),**3.93-3.89**(d, appear as sharp singlet ,3H, $N(+)CH_3$), **1.888**(m,2H,$NCCH_2$) **1.296-1.419**(m, 2H, $NCCCH_2$), **0.959**(t,3H,NCCCCH3); **$BMPyBF_4$ in $CDCl_3$(δ/ppm)**: 3.57-3.62(t,2H, $SOCH_2$); 3.45(ss,4H,CH_2NCH_2); 3.4(t,2H,NCH_2C) ; 3.096 (s,3H,CH_3N); 2.2(s, 4H,CCH_2CH_2C), 1.763(m, 6H, $NCCH_2CC$ & 4 ring protons opposite to N i.e. $H_2CCNCCH_2$); 1.73(m, 2H,$NCCH_2C$); 1.403(m, 2H, $NCCC\underline{H_2}CH_3$); 1.2(m, 20H, $(CH_2)_{10}$); 0.978 (t, 3H, $NCCCC\underline{H_3}$) ; 0.92(t, 3H, $NCCCCH_3$); **SDS in D_2O (7.5mM):** (δ/ppm): 4.711(m, HOD), 3.958 (t, 2H, $SO\underline{CH_2}$), 1.188(m, appear as s, 16H, $[CH_3\underline{(CH_2)_8}CH_2CH_2CH_2SO]$, 1.579(m, appear as triplet, 4H, $SOCH_2\underline{CH_2CH_2}$), 0.78-0.757(t, $\underline{CH_3}(CH_2)_{10}CH_2SO$); **SDS in D_2O (5mM):** (δ/ppm): 4.711(m, HOD), 3.96 (t, 2H, $SO\underline{CH_2}$), 1.181(m, appear as s, 16H, $[CH_3\underline{(CH_2)_8}CH_2CH_2CH_2$ SO], 1.58(m, appear as triplet, 4H, $SOCH_2\underline{CH_2CH_2}$), 0.78-0.737(t, $\underline{CH_3}(CH_2)_{10}CH_2$ SO).

The outcome of ^{1}H NMR of **BMIMDS and BMPDS** are given as follows: **BMIMDS D_2O below CMC (δ/ppm):** 7.307(doublet, 2H, NCH), 4.077(t, 2H, NCH_2), 3.952(t, 2H, $SOCH_2$), 3.769 [sharp singlet, 3H, $N(+)CH_3$], 1.75 (m,2H, $NCCH_2$), 1.55 (t, 2H, $NCCCH_2$), 1.21 (m, J = 9 Hz, $SOCH_2(C\underline{H}_2)_9$, 20H), 0.80(m,3H, $NCCCC\underline{H}_3$ & 3H, $SOC_{11}C\underline{H}_3$)[below CMC]; **$CDCl_3$ above CMC** (δ/ppm): 9.57 (s, 1H, NCHN), **7.33,7.43**(d, 2H, NCH), **4.245**(t, 2H, NCH_2), **4.132** (t, 2H, $SOCH_2$), **2.795** [s, 3H, $N(+)CH_3$], **2.051**(s, 6H, acetone impurity), **1.89** (m,2H, $NCCH_2$), **1.665** (t, 2H, $NCCCH_2$), **1.35** (m, J = 9, $SOCH_2(C\underline{H}_2)_9$, 20H), **0.955**(t, J = 7.35, 3H, $NCCCC\underline{H}_3$), **0.876**(t, 3H, $SOC_{11}C\underline{H}_3$). 2 signals appear together as multiplet as both triplets are in the same zone.

BMPDS in $CDCl_3$ For ^{1}H NMR (δ/ppm): 3.94(t,2H, $SOCH_2$), 3.45(ss,4H,CH_2NCH_2), 3.4(t,2H,NCH2C), 3.2(s,3H,CH_3N+), 2.2(s, 4H,CCH_2CH_2C), 1.73(m, 2H,$NCCH_2C$), 1.6(m, 2H, $NCCCH_2C$), 1.2(m, 20H, $(CH_2)_{10}$), 0.92(t, 3H, $NCCCCH_3$), 0.83(t, 3H, CH_3).

BMIMDS in $CDCl_3$ for 13C NMR (δ/ppm): 137.80 (1C, NCHN), 123.52(+NCHCH), 122(+NCHCH), 77.5, 77.07, 76.65($CDCl_3$), 67.85($SOCH_2$) due to shielding after micellization,49.81($N\underline{C}CCCH_3$),36.47($+NCH_3$),32.09($NC\underline{C}CCH_3$),31.93($SOCH_2(CH_2)8CH_2$), 29.66($SOCH_2CH_2CH_2(CH_2)_5$), 29.55($SOCH_2CH_2$ $CH_2(CH_2)_5$ CH_2CH_2), 29.43($SOCH_2CH_2$), 25.91($SOCH_2CH_2$ CH_2), 22.71($SOCH_2CH_2$ $CH_2(CH_2)_5$ CH_2 CH_2CH_2), 19.46($NCC\underline{C}CH_3$), 14.16($SO(CH2)_9$ $CH_2CH_2CH_3$), 13.44($NCCCCH_3$).

BMPDS in $CDCl_3$ for ^{13}C NMR (δ/ppm): 77.54, 77.12, 76.69($CDCl_3$), 67.61($SOCH_2$), 64.23,64.13($+N(CH_2)_2$), 48.18($+NCH_3$), 31.87{$SOCH_2(CH_2)8CH_2$}, 29.31($SOCH_2CH_2$), 29.60{$SOCH_2CH_2CH_2(CH_2)$},29.39{$SOCH_2(CH_2)_7CH_2$},25.88($SOCH_2CH_2CH_2$),25.68{$SOCH_2$ $(CH_2)_9CH_2$}, 22.65($NCCCCH_3$), 21.56($+N(CH_2)_2(CH_2)_2$), 19.64($NCCCCH_3$), 14.10($NCCCCH_3$), 13.53{$SO_2CH_2)_9$ $CH_2CH_2CH_3$} .

^{1}H NMR of SDS in D_2O below CMC

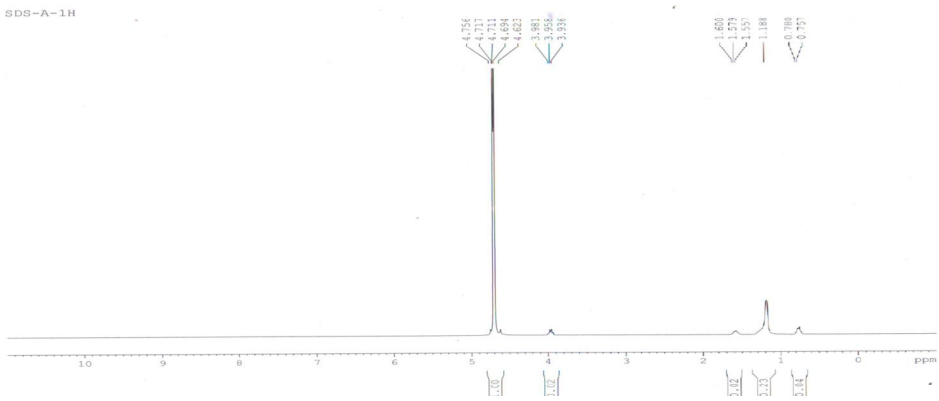

^{1}H NMR of SDS in D_2O below CMC

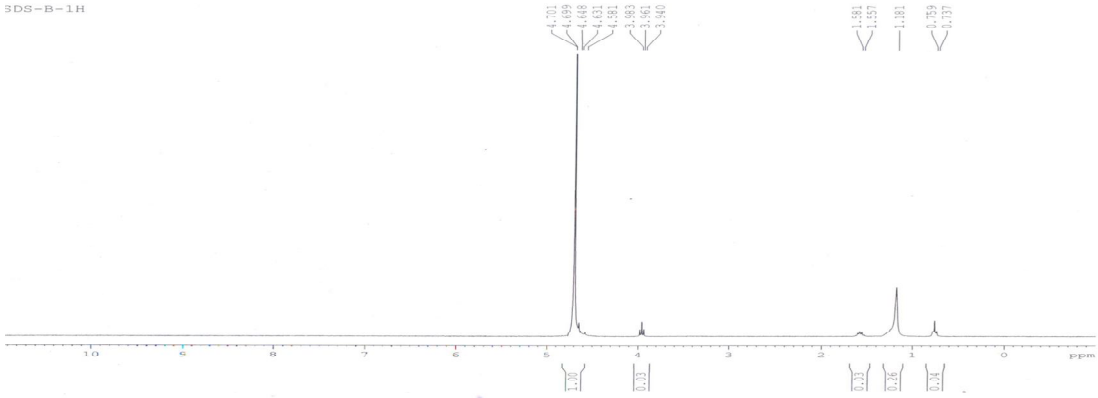

^{1}H NMR of BMIMCl in D_2O

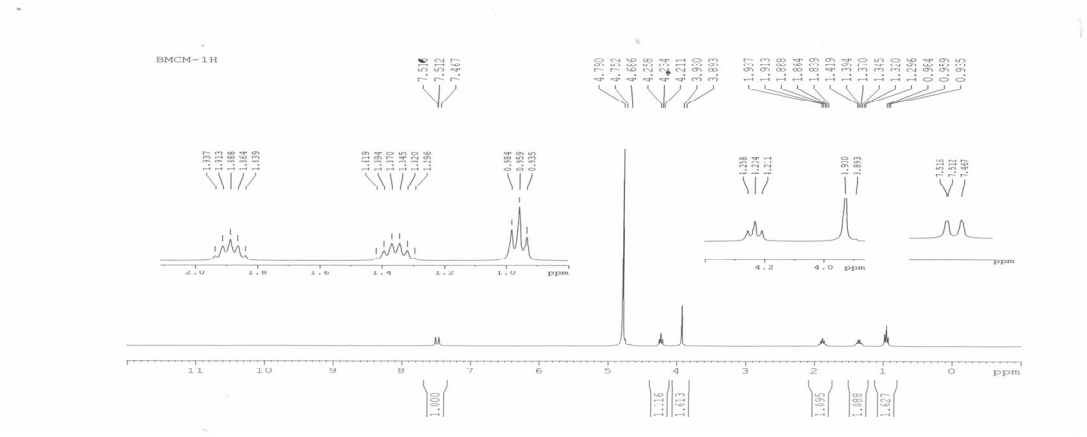

NMR of $BMPyBF_4$ in $CDCl_3$

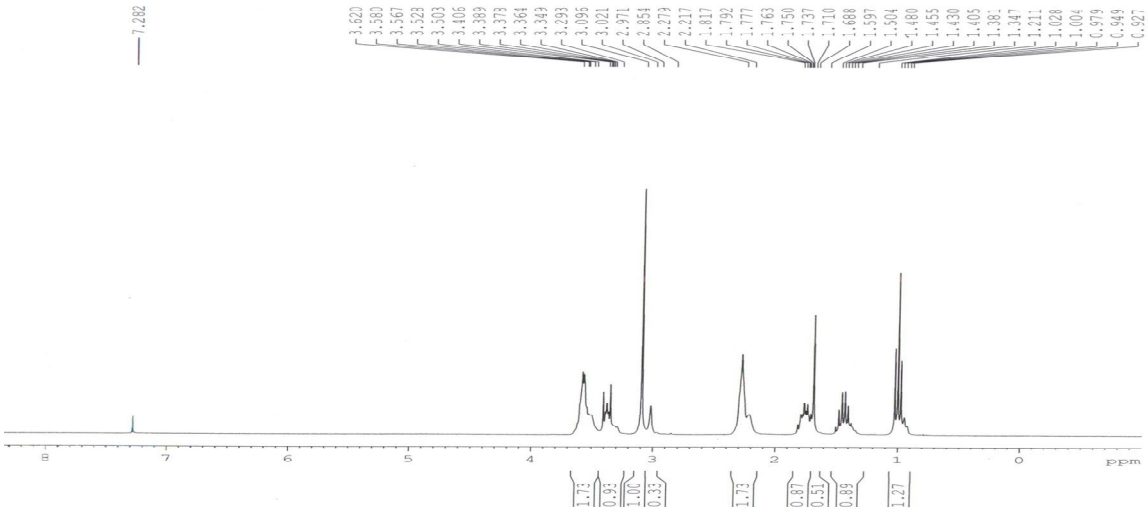

Characterization: 1H NMR of BMIMDS in $CDCl_3$

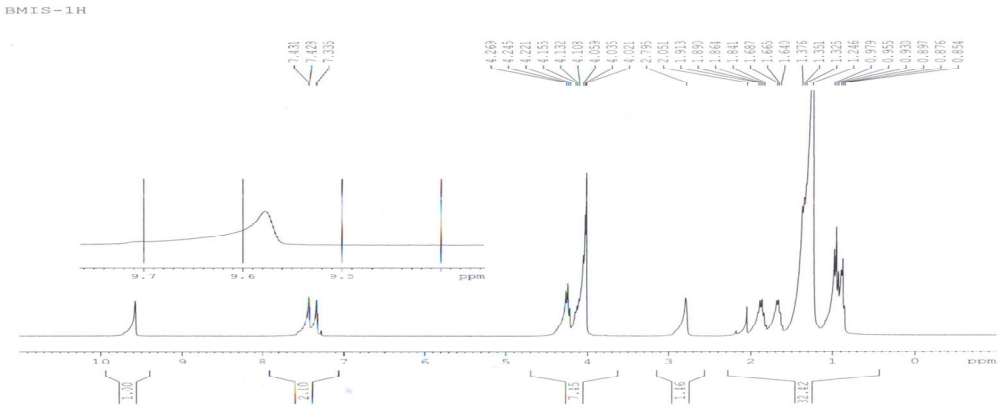

Characterization: ^1H NMR of BMIMDS in D_2O below CMC

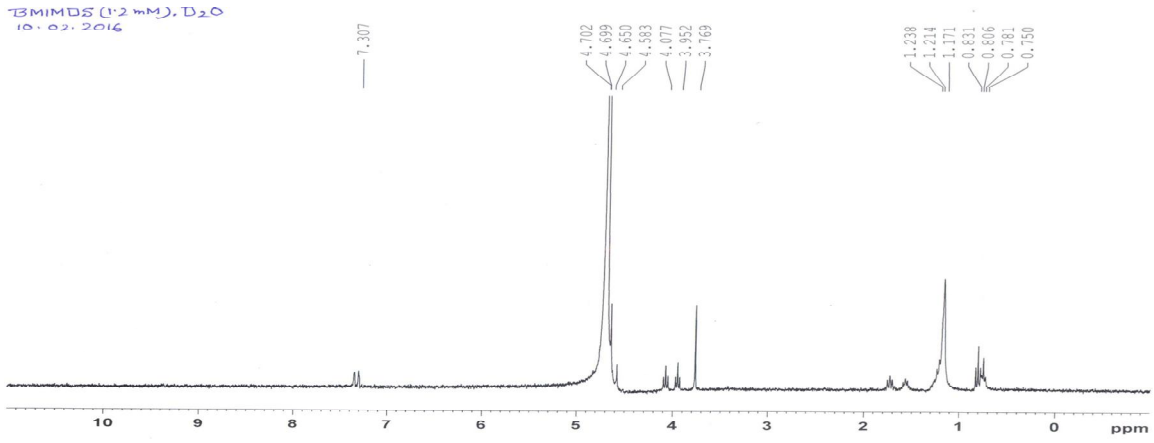

C-13 NMR of BMIMDS in $CDCl_3$

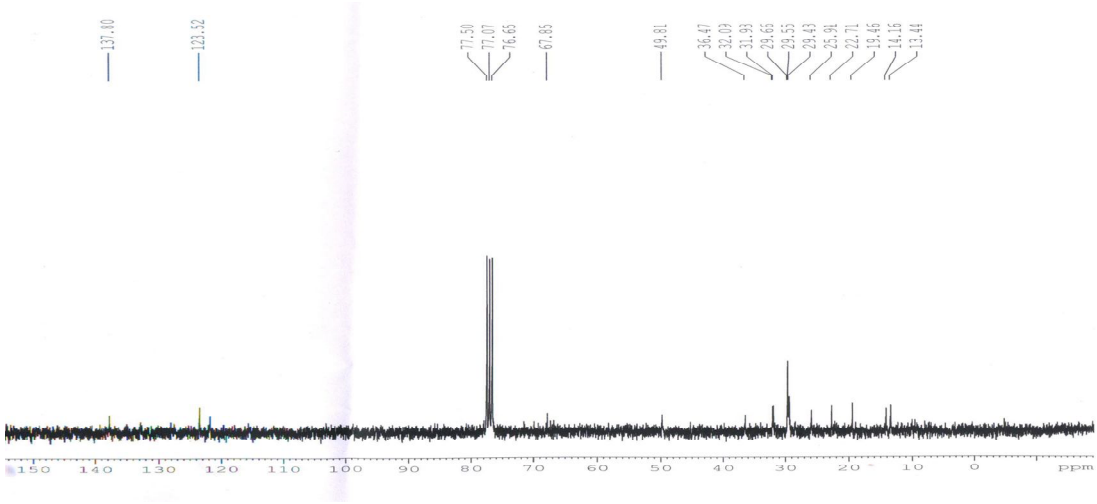

1H NMR of BMPDS in $CDCl_3$(128S)

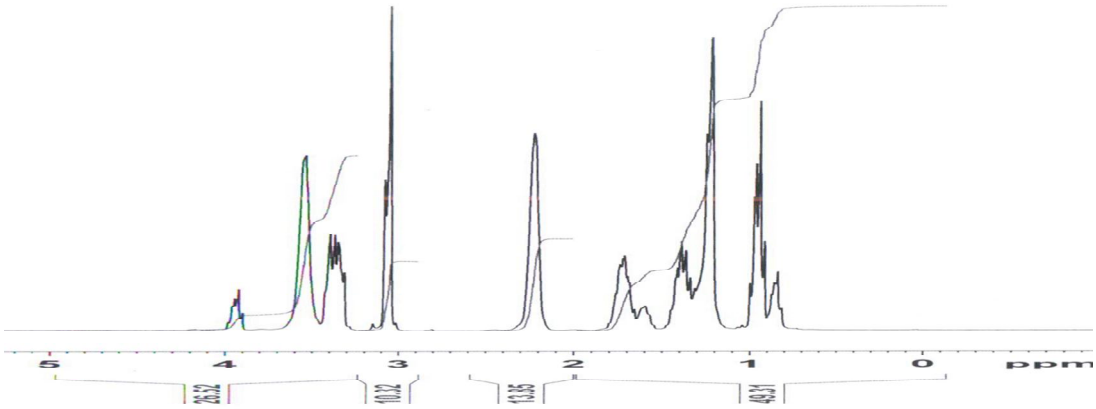

C-13 NMR of BMPDS in $CDCl_3$

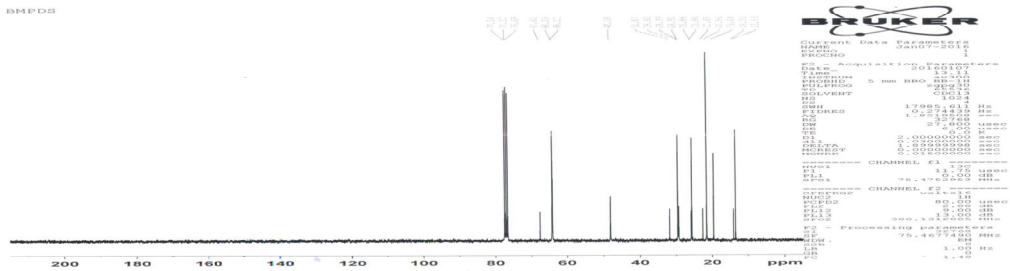

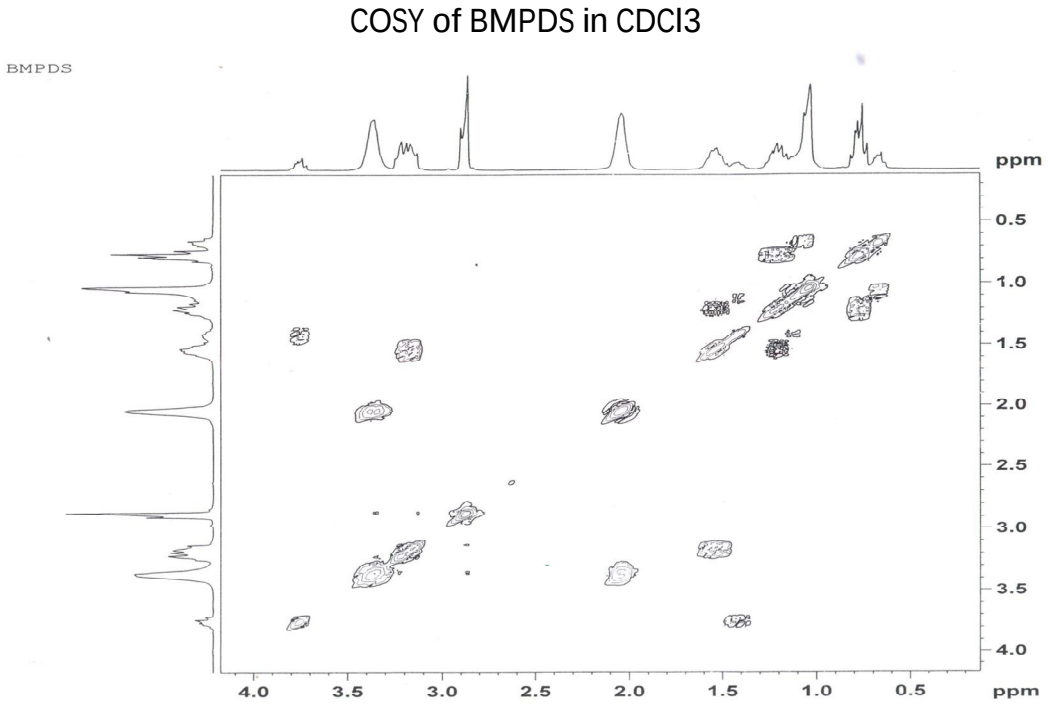

Fig. 2. ^{1}H NMR spectra of SDS, BMIMCl, BMPyBF$_4$, BMIMDS and BMPDS; ^{13}C NMR spectra of BMIMDS and BMPDS; 2D COSY spectra of BMPDS.

5.2.6 Purity check by melting point: The purity of all the precursor and the products were also checked by melting point. The obtained data for the melting point are given below.

Serial no.	Sample name	Melting point(^{o}C)
1.	SDS	195-200
	SDS R	206
2.	BMPyBF4	158
3.	BMIMCl	70
4.	BMIMDS	43
5.	BMPDS	Viscous liquid

Table 2: Melting point of the 3 precursors & 2 synthesized compounds

5.3. Study of physicochemical properties of BMIMDS and BMPDS:

5.3.1. CMC determination

5.3.1.1. Conductance:

The critical micelle concentration (CMC) is a thin concentration range where the physical properties of the solution of an amphiphile show a sudden change due to the cooperative formation of micelles or other type of aggregate in the bulk solution. [35]
The CMC value is obtained from the intersection of two straight lines, which was drawn by the principle of best fitting from the most frequent data. From the conductometric curve (Fig. 3) the CMC value of BMIMDS & BMPDS obtained was 2.53 and 2.91 milimolar was quite less than the common precursor SDS. Therefore BMIMDS & BMPDS has more efficient surface activity compared to its anionic surfactant (SLS).

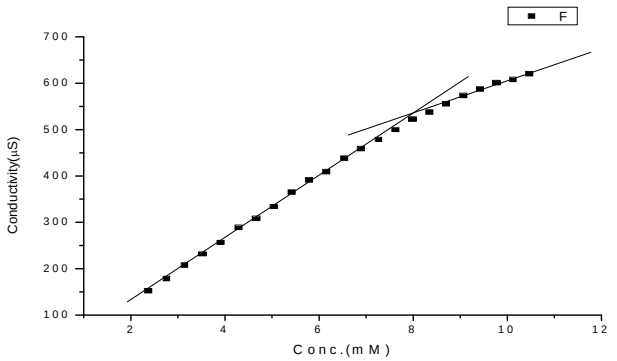

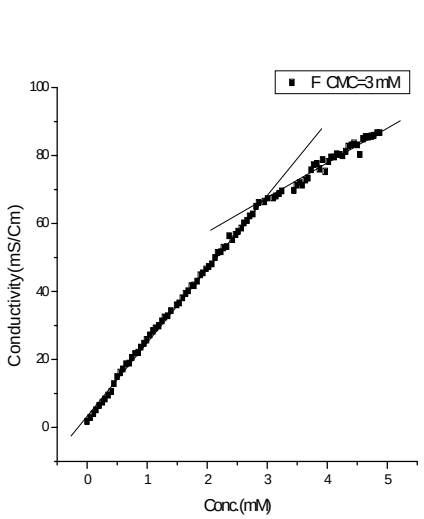

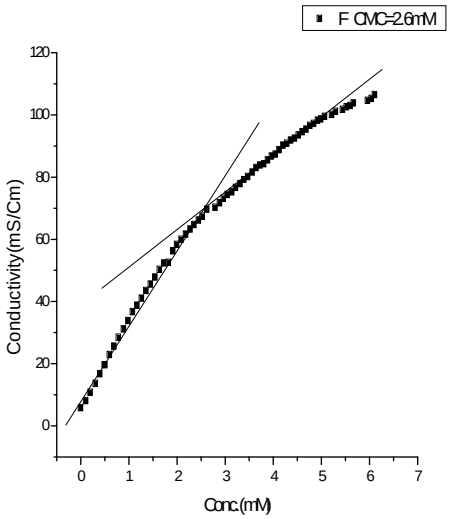

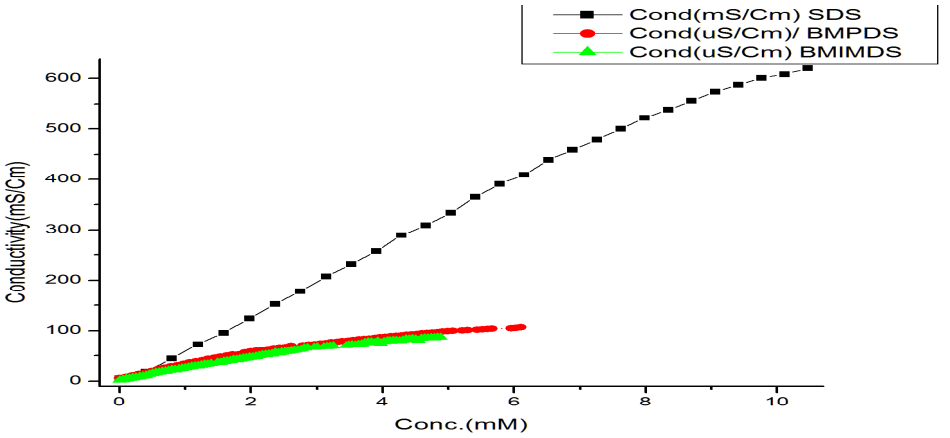

Fig.3. Specific conductance vs. conc. (mM) of SDS, BMIMDS & BMPDS respectively for CMC determination; all the graphs in same place for comparison

5.3.1.2. Surface tension: Surface tension measurements were performed to assess the surface activities of synthesized SAILs in aqueous solution. The plots of surface tension (γ) at 25^{o}C (298K) versus log C for BMIMDS & BMPDS are depicted in Fig. 3. The surface tension of aqueous solutions linearly decreases with the logarithm of concentration to a certain value, above which a nearly constant value of surface tension (γ_{cmc}) is observed. The absence of a minimum around the breakpoint demonstrates the high purities of these SAILs. The breakpoint connecting the two regions corresponds to the critical micelle concentration (CMC) value. The CMC values for BMIMDS & BMPDS are listed in Table 3.a., together with the data reported for SDS. [36], [37], [20]

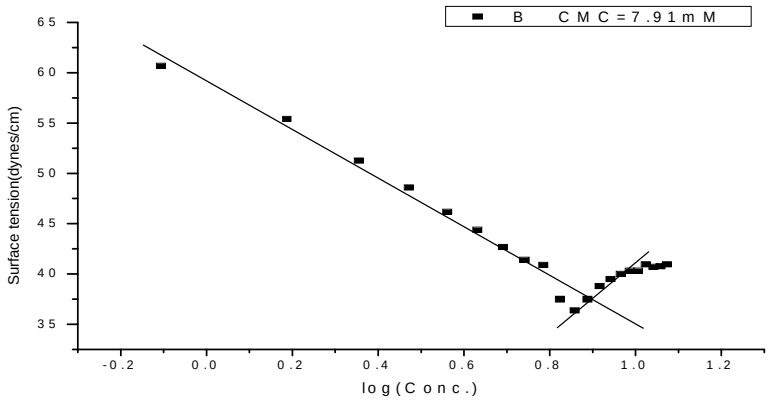

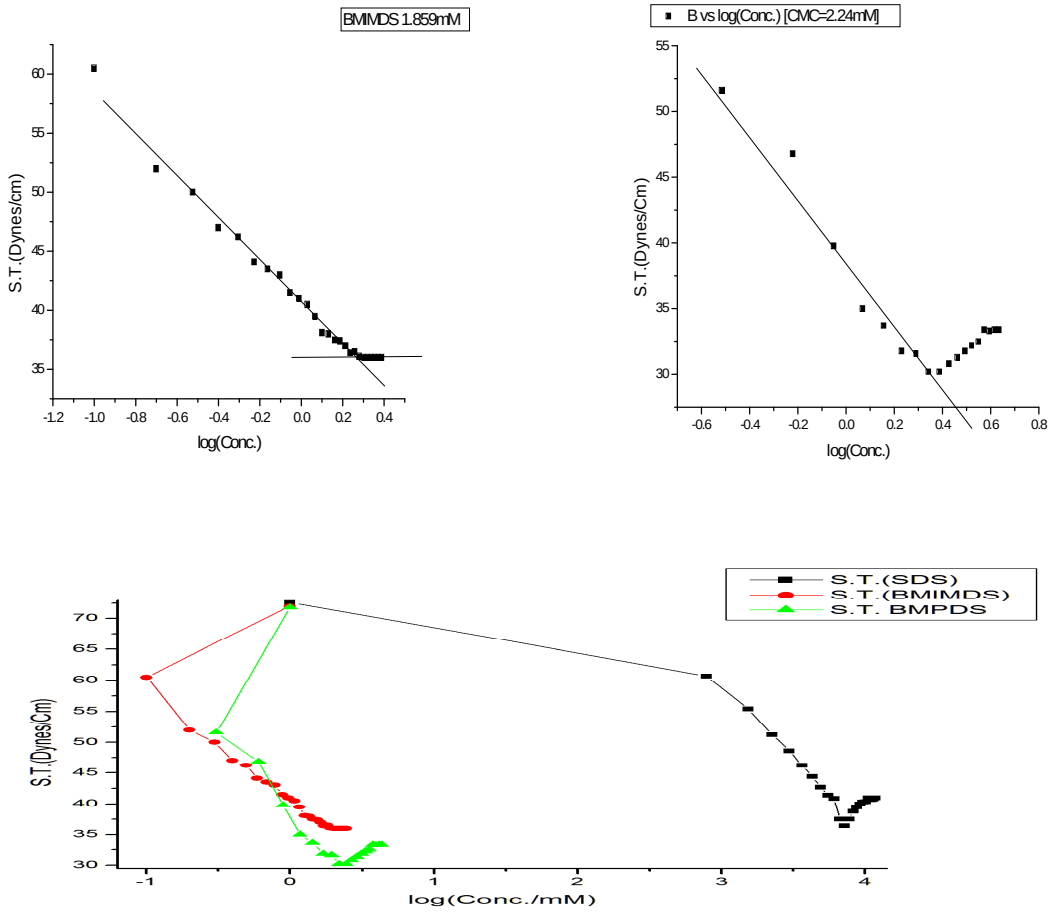

Fig. 4. Surface tension vs. log (conc.) (mM) of SDS, BMIMDS & BMPDS respectively for CMC determination; the entire graph in same place with colour caption for easy comparison

5.3.2. Fluorescence, static Fluorescence Quenching and Average Aggregation Number:

The CMC value of surfactant can be determined quite easily from the measurements of the fluorescence intensity in surfactant solution using polarity probe pyrene, where surfactant itself is fluorescence inactive. [38]

The CMC measurement was done by steady-state fluorescence technique. Initially, blank pyrene solution was taken in the cuvette and gradually surfactant containing

pyrene solution was added. From the graph, the value of CMC obtained was 2 & 2.15 (Fig. 5 & 6) which is quite close to the values obtained from the conductance study (Table 3. a.).

The aggregation number (n) was obtained was 40 & 42 for BMIMDS & BMPDS respectively from the fluorescence. The quencher used for the fluorescence was cetyl pyridinium chloride (CPC). (Fig. 5 & 6) (Table 3. b.).

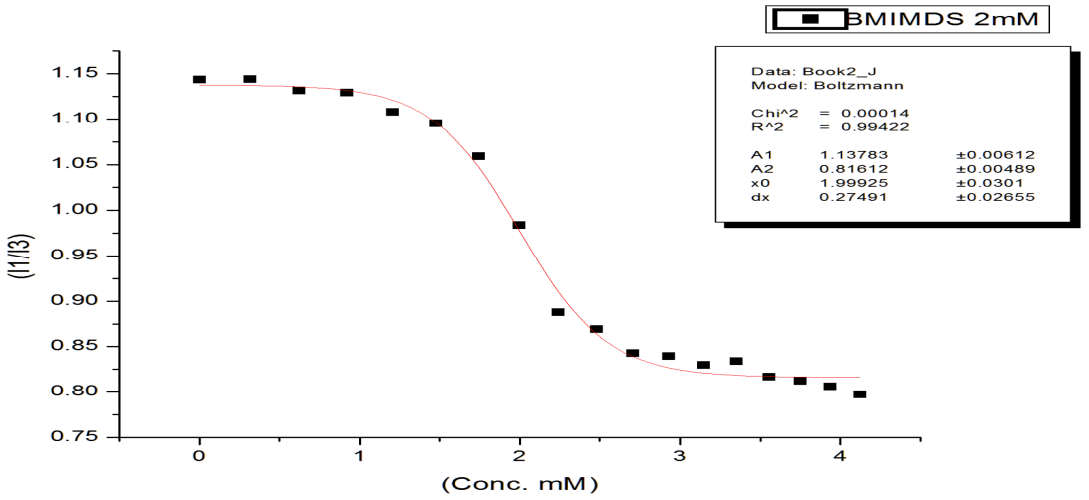

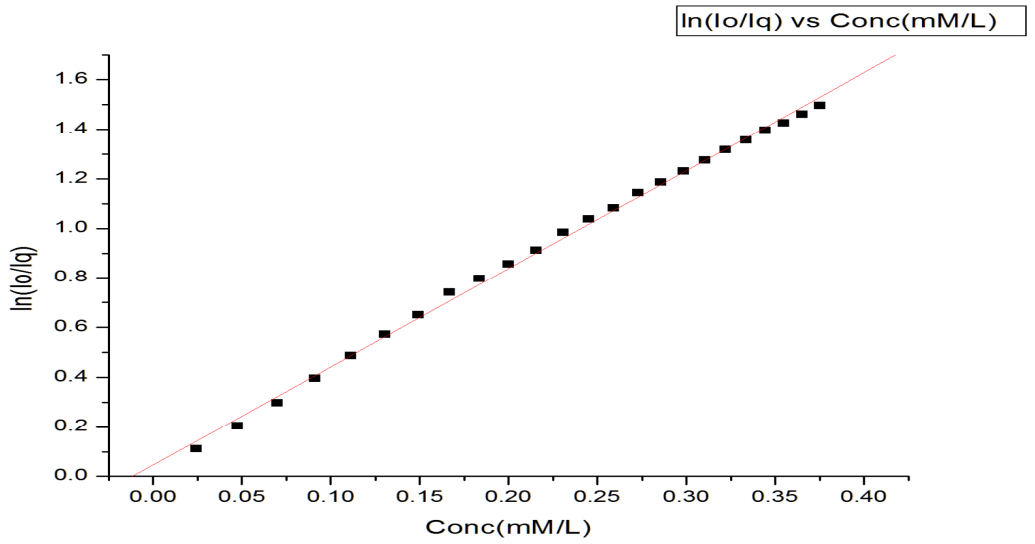

Fig. 5. Fluorimetric determination of CMC of the BMIMDS & and its ln (I_0/Iq) vs. Conc. (mML^{-1}) of quencher graph.

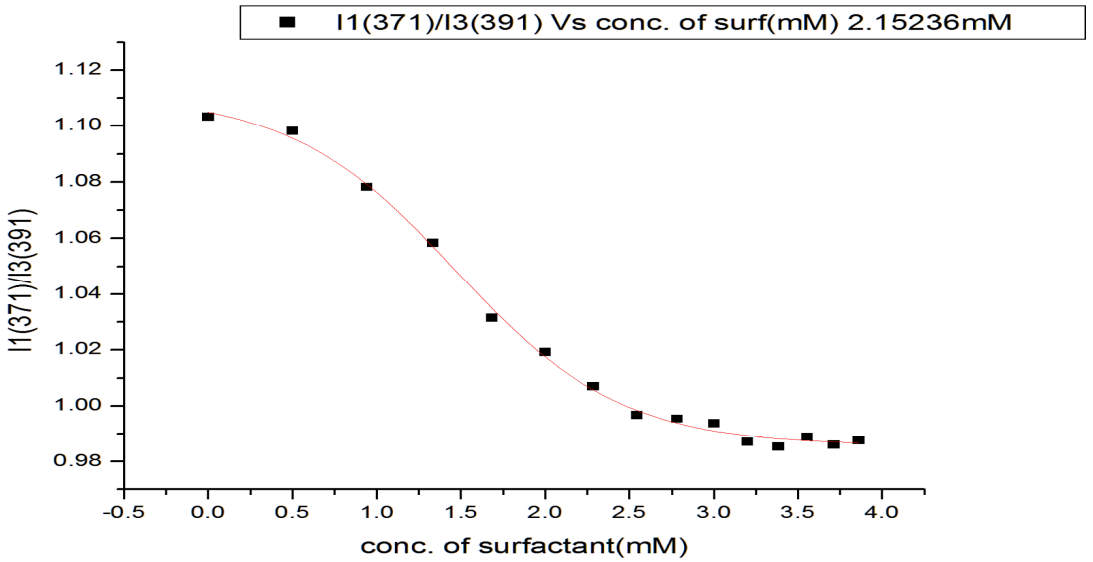

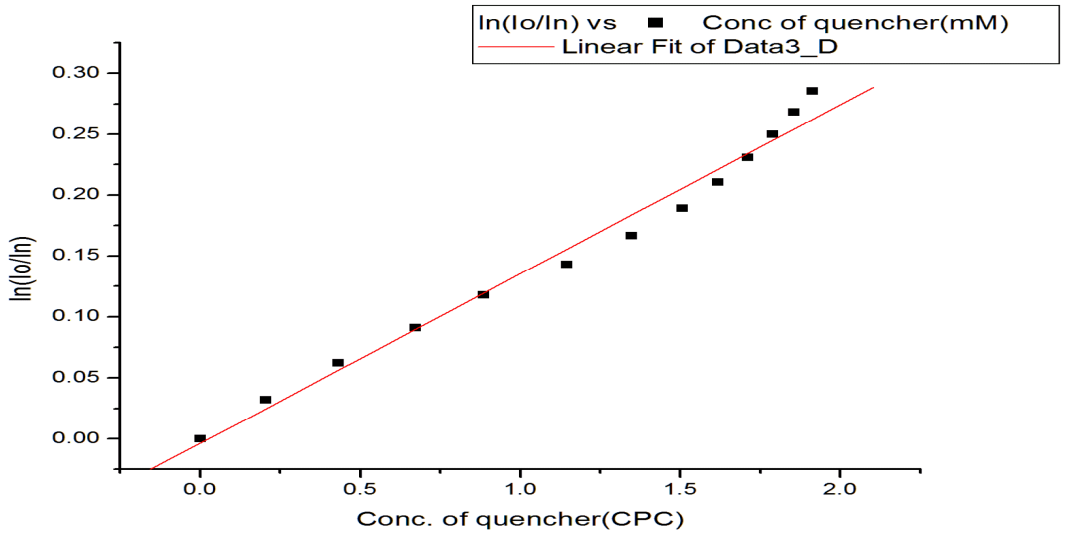

Fig. 6. Fluorimetric determination of CMC of the BMPDS & and its ln (I_0/Iq) vs. Conc. (mML^{-1}) of quencher graph.

Surfactants	CMC values(mM) Conductometrically	CMC values(mM) Surface tensiometrically	CMC values(mM) Fluorimetric technique	JPC(B)
SDS	8.1	7.91(7.8)*	7.2	7.8
BMPDS	2.53(3.8)*	2.29(2.7)*	2.15	3.8 & 2.7
BMIMDS	2.97(2.1)*	1.87(1.8)*	2	2.1 & 1.8

a)

Surfactant name	CMC values	Aggregation number (n)
BMIMDS	2	42
BMPDS	2.15	40

b)

Table 3: a) The CMC values of SDS, BMIMDS & BMPDS by three different techniques

b) The CMC values & aggregation number of BMIMDS & BMPDS from fluorescence

5.3.3. DSC study: DSC study was done in the case of SDS, given 2 significant peaks before and just before its melting point. (Fig. 7.).

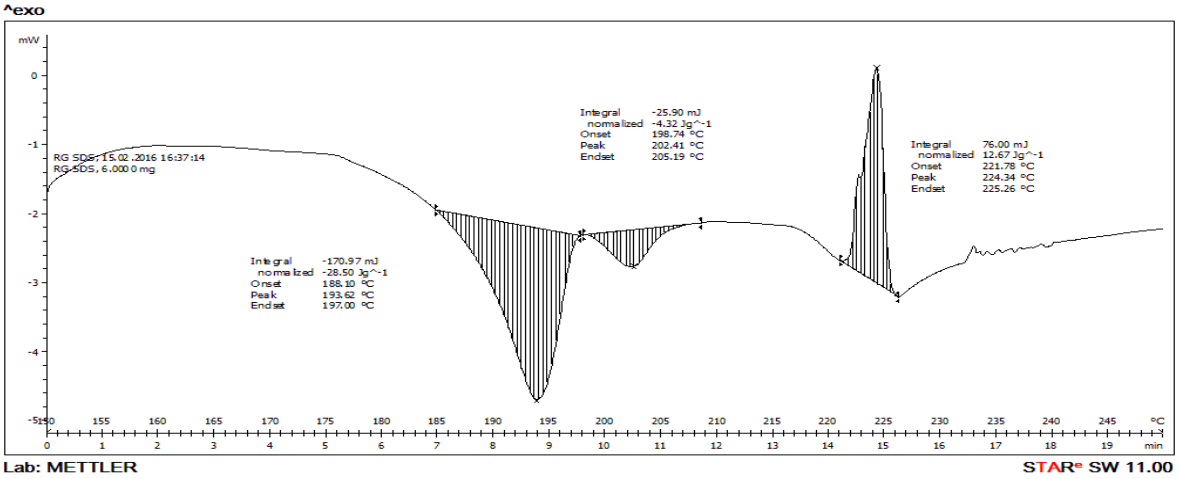

Fig. 7. DSC thermo gram of the SDS (recrystallized)

5.3.4. POM study: POM study of the BMIMDS show lamellar behavior obtained similar to liquid crystal. POM images of the BMPDS were taken at different temperature. With increase in temperature the aggregate nature was disappear for the BMPDS. [39]

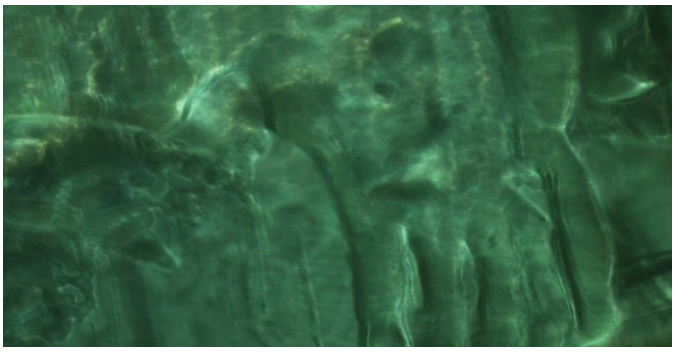

Fig. 7. a. **POM image of BMIMDS**

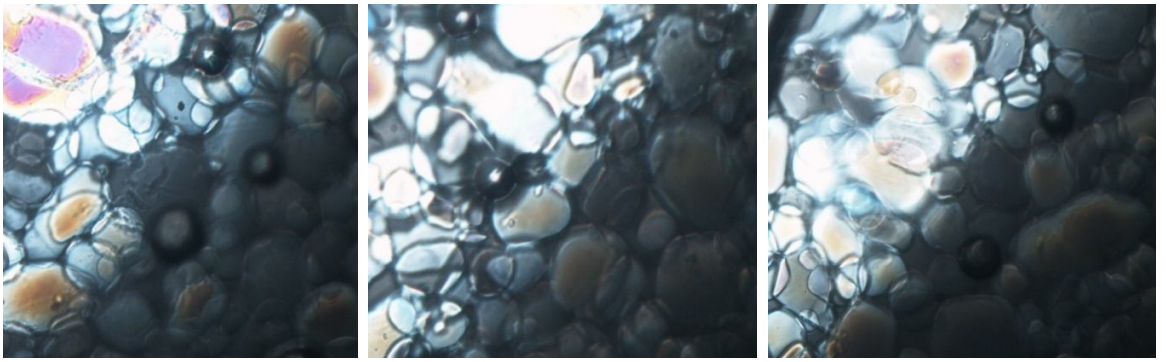

Fig. 7. b. **POM image of the BMPDS at different temperature**

5.3.5. DLS Study: In DLS the size distribution of molecules or particles is the property of significance. Here, the distribution explains how much material there is nearby of the different size "slices." In DLS, the local distribution is the concentration distribution which indicates how much light is scattered from the various size "slice" or "bins". Historically, a simpler forced single exponential fitting method (the cumulant method) has been used to find an overall mean size (by intensity) and an overall polydispersity (the normalized next cumulant). Traditionally, this overall polydispersity has also been converted into an overall polydispersity index PDI which is the square of the light scattering polydispersity. For a perfectly uniform sample, the PDI would be around 0.0. We had obtained the average PDI value of 0.711 which indicate broad poly dispersity of the inclusion complex, supported by HRTEM [40, 41]. Higher value of zeta potential of BMIMDS compare to BMPDS at comparable concentration established role of counter ion in monomer as well as micellar stability. Equivalent size profiles from DLS for both derived surfactants indicate the aggregation even far beyond CMC. [Fig.8.a)- c)]

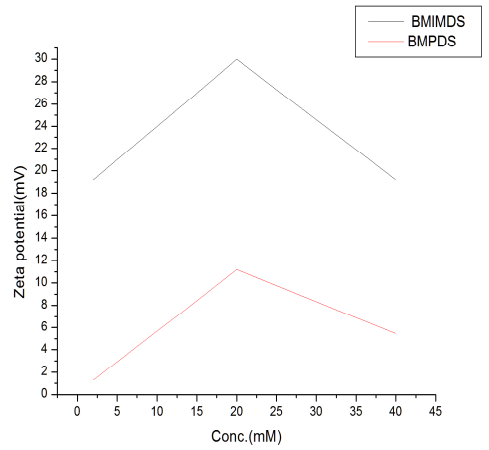

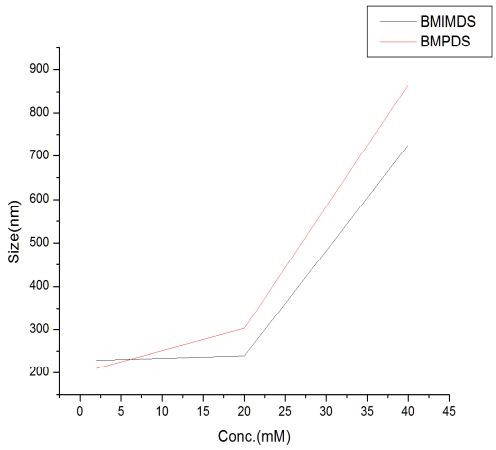

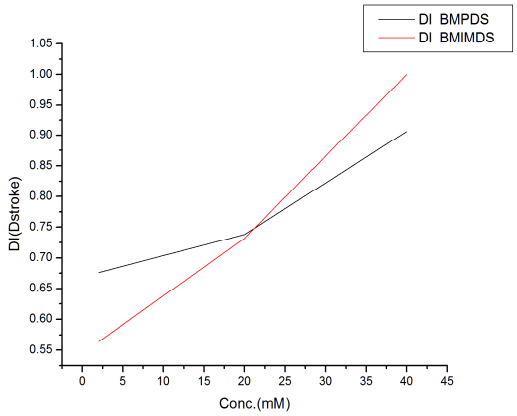

Fig.8.a). Comparison of change of the Zeta potential with concentration of BMIMDS & BMPDS

Fig. 8. b). Comparison of change of the size with concentration of BMIMDS & BMPDS

Fig. 8. c). Comparison of change of the dispersity with concentration of BMIMDS & BMPDS

5.4. Conclusions: Benign ionic liquid based surfactants were synthesized. Melting point, FTIR, FTNMR was confirmed about the purity of the product. The CMC value obtained from 3 techniques implies BMIMDS has lower CMC and higher efficiency as surfactant than BMPDS. BMIMDS & BMPDS has quite similar aggregation number, obtained from the fluorescence quenching method**.** Higher value of zeta potential of BMIMDS compare to BMPDS at comparable concentration established role of counter

ion in monomer as well as micellar stability. Equivalent size profiles from DLS for both derived surfactants indicate the aggregation even far beyond CMC. POM study of the BMIMDS show lamellar type behavior obtained similar to liquid crystal. With increase in temperature the aggregate nature was disappear for the BMPDS.